Available online at www.sciencedirect.com
ScienceDirect
International Journal of Heat and Mass Transfer 51 (2008) 3434–3441
International Journal of HEAT and MASS TRANSFER
www.elsevier.com/locate/ijhmt

Inverse radiation problem of temperature field in three-dimensional rectangular enclosure containing inhomogeneous, anisotropically scattering media

D. Liu, F. Wang *, J.H. Yan, Q.X. Huang, Y. Chi, K.F. Cen

State Key Laboratory of Clean Energy Utilization, Zhejiang University, Hangzhou 310027, People's Republic of China

Received 28 June 2007; received in revised form 29 October 2007
Available online 24 March 2008

Abstract

An inverse radiation analysis is presented for determining the three-dimensional temperature field in an inhomogeneous, absorbing, emitting and anisotropically scattering media of known radiative properties from the knowledge of the exit radiative energy received by charge-coupled device (CCD) cameras at boundary surfaces. The forward Monte Carlo method was employed to describe the radiative energy propagation. The inverse problem was formulated as an ill-posed matrix equation and solved by least square QR decomposition (LSQR) method. The measured data were simulated by adding random errors to the exact solution of the direct problem. The effects of measurement errors, combinations of CCD cameras, concentration distributions of particles, and coefficient fluctuating errors on the accuracy of the inverse problem were investigated. The results show that the three-dimensional temperature field can be estimated accurately, even for the noisy data.

Keywords: Inverse radiation problem; Temperature field; Charge-coupled device; Least square QR decomposition

1. Introduction

Thermal radiation is the dominant heat transfer mode in high temperature devices such as combustion chambers and furnaces. A comprehensive review of radiative heat transfer in combustion systems has been given by Viskanta and Mengüç [1].

Inverse analysis of radiative transfer is concerned with the determination of the radiative properties, boundary conditions and the temperature field or source term distribution from different kinds of radiation measurements. A thorough review of inverse radiation problems has been given by McCormick [2]. A lot of work has been reported on the estimation of radiative properties [3–10]. Many researchers have also dealt with the inverse problems for determining the temperature profile or source term in media. Li and Özişik [11,12], Siewert [13,14], Li [15] and Liu [16–18] have reconstructed the temperature profiles or source terms in plane-parallel, spherical, and cylindrical media by the inverse analysis form the data of the radiation intensities exiting the boundaries. Li [19,20] considered the estimation of the unknown source term in two-dimensional absorbing, emitting, and scattering rectangular and cylindrical medium. However, only few studies have been carried out on the determination of the temperature profile or source term in three-dimensional participating media. Inverse radiation analysis of estimating three-dimensional temperature field or source term has been given by Liu [21,22], who used conjugate gradient method that minimized the error between the calculated exit radiative intensities and the experimental data.

The forward Monte Carlo method was employed to describe the radiative energy propagation in this paper. The comprehensive review of Monte Carlo method in

* Corresponding author. Tel.: + 86 571 87952628; fax: + 86 571 89752438.
E-mail address: wangfei@cmee.zju.edu.cn (F. Wang).

0017-9310/$ - see front matter © 2007 Published by Elsevier Ltd.
doi:10.1016/j.ijheatmasstransfer.2007.11.007

Nomenclature

$\boldsymbol{A}$	coefficient matrix in Eq. (11)
$\boldsymbol{A}_{\mathrm{err}}$	coefficient matrix with errors
$A_{\mathrm{err},n}$	element of coefficient matrix $\boldsymbol{A}_{\mathrm{err}}$
A_n	element of coefficient matrix $\boldsymbol{A}$
$D_{i\to j}$	radiative energy fraction
$\boldsymbol{E}$	radiative energy vector
$\boldsymbol{E}_{\mathrm{measured}}$	energy vector with errors
$E_{\mathrm{measured},j}$	element of the energy vector $\boldsymbol{E}_{\mathrm{measured}}$
E_j	the element of energy vector $\boldsymbol{E}$
f_j	energy propagation and imaging process
M	number of pixels
N	number of volume elements
P_j	radiative energy received by each pixel
T_i	temperature of volume element i
$\boldsymbol{T}_E$	unknown in Eq. (11)
T_i^{recon}	reconstructed temperature
T_i^{exact}	exact temperature
ΔV_i	volume of volume element i

Greek symbols

σ_0	Stefan–Boltzmann constant
μ	average value in Eqs. (12) and (13)
$\alpha_{\mathrm{g},j}$	gas absorption coefficient
$\alpha_{\mathrm{p},i}$	particle absorption coefficient
σ_1	mean square deviation in Eq. (12)
σ_2	mean square deviation in Eq. (13)
λ_1	minimum wavelength
λ_2	maximum wavelength
α_i	Planck mean absorption coefficient
ψ	scattering angle

Subscripts

i	volume number
j	pixel number
n	number of elements in Eq. (13)

radiative heat transfer has been given by Howell [23]. The validity of the Monte Carlo method used in this work has been proved by comparing our results with those in literatures [24,25].

The accurate, convenient and noncontact determination of temperature field is important for the study of combustion science. In the present study, we develop a method of solving three-dimensional inverse radiation problem which allows one to determine the three-dimensional temperature field in an inhomogeneous, absorbing, emitting and anisotropically scattering media of known radiative properties from the knowledge of the exit radiative energy received by charge-coupled device (CCD) cameras at boundary surfaces. Based on Monte Carlo method, the inverse problem was formulated as an ill-posed matrix equation and solved by LSQR method. The measured data were simulated by adding random errors to the exact solution of the direct problem. At present, from the point of view of application in practice, it should be possible to provide approximately reasonable radiative properties, such as absorption and scattering coefficients in combustion system, based on some references such as [1,26–29] and some CFD simulation results.

The effects of measurement errors, combinations of CCD cameras, concentration distributions of particles, and coefficient fluctuating errors on the accuracy of the inverse problem will be examined.

2. Analysis

2.1. Model description

The direct problem of concern here is to find the exit radiative energy received by CCD cameras at the boundary surfaces for the known temperature field and radiative properties.

The system under consideration is depicted in Fig. 1, which is a rectangular enclosure containing participating media. The participating media used in literatures [24,25] is adopted as the media analyzed in this study, which is an inhomogeneous, absorbing, emitting and anisotropically scattering medium in the rectangular, cold and black enclosure, with dimensions W, L, H of the x-, y- and z-directions. The center of coordinate system is in the center of the enclosure. The system is assumed to be divided into $7\times7\times7$ volume elements in three dimensions. The medium consists of a mixture of nitrogen and carbon dioxide gases plus varying concentration of carbon particles. Two kinds of concentration distributions of carbon particles are assumed, as shown in Fig. 2. The serial

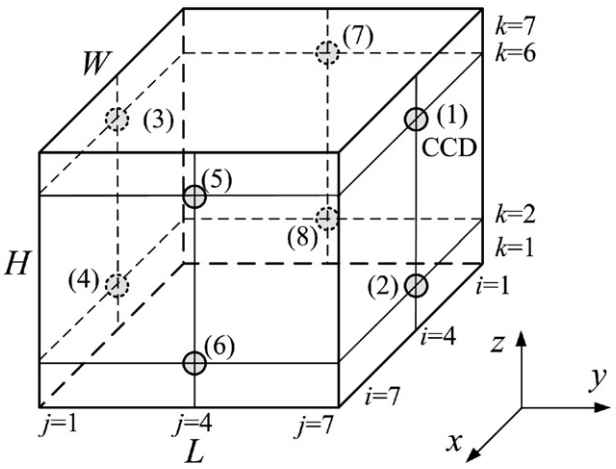

Fig. 1. Coordinate system and dimensions for three-dimensional rectangular enclosure.

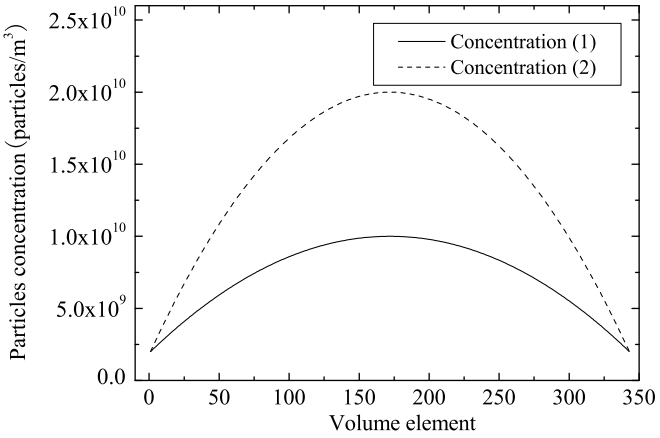

Fig. 2. Two kinds of concentration distributions of carbon particles.

number $1,2,\ldots,343$ of the abscissa is as the following sequence (i,j,k): $(1,1,1),(2,1,1),\ldots,(7,1,1),(1,2,1),(2,2,1),\ldots,(7,7,1),(1,1,2),\ldots,(7,7,7)$, as shown in Fig. 1. The total mixture pressure is specified to be 1atm, with a volume fraction of carbon dioxide of 0.21. The carbon particles are specified to be of uniform diameter, 30 μm. In order to obtain the exit radiation information, eight CCD cameras are used and mounted at the boundary surfaces, as shown in Fig. 1.

The radiative properties of carbon particles can be calculated by Mie theory [26] and the carbon particles exhibit highly forward scattering behavior. The scattering phase function is assumed to be adequately approximated by the gray delta-Eddington function given as [24,25,30]

$$\Phi(\psi) = 2f\delta(1-\cos\psi) + (1-f)(1+3g\cos\psi) \tag{1}$$

where f and g quantify the forward scattering behavior and were specified to be 0.111 and 0.215, respectively.

In the present work, the walls are assumed to be cold. Wall temperatures are much lower than those in the furnace so the radiative energy emitted by the walls can be ignored. Let N be the total number of volume elements. CCD camera target plane is assumed to be divided into M pixel elements. Monte Carlo method is employed to describe the radiative heat transfer and M equations can be obtained

$$\begin{aligned} f_1(T_1,T_2,\ldots,T_N) &= P_1 \\ f_2(T_1,T_2,\ldots,T_N) &= P_2 \\ &\vdots \\ f_M(T_1,T_2,\ldots,T_N) &= P_M \end{aligned} \tag{2}$$

where P_j is the radiative energy received by each pixel on the CCD target plane, f_j represents radiative energy propagation and imaging process which can be obtained by Monte Carlo method, T_i is the temperature of each volume element i, $j=1,2,\ldots,M$, $i=1,2,\ldots,N$.

Within the response wavelength range of CCD camera, the energy emitted by volume element i was calculated by

$$E_i = 4\alpha_i\sigma_0\Delta V_i\cdot T_i^4 \tag{3}$$

where α_i is Planck mean absorption coefficient of volume element i, σ_0 is Stefan–Boltzmann constant, ΔV_i is the volume of volume element i.

The radiative energy arriving at the pixel j on the CCD target plane from the total energy emitted by the volume element i is

$$E_{i\to j} = E_i\cdot D_{i\to j} \tag{4}$$

where $D_{i\to j}$ is the radiative energy fraction of total energy emitted by volume element i, received by pixel j on the CCD target plane.

Within the response wavelength range of CCD camera, Planck mean absorption coefficient was calculated by the following equation:

$$\alpha_i = \frac{\int_{\lambda_1}^{\lambda_2}(\alpha_{g,i}+\alpha_{p,i})e_{b\lambda,i}\,d\lambda}{\sigma_0 T_i^4} \tag{5}$$

where $\alpha_{g,i}$ and $\alpha_{p,i}$ are gas absorption coefficient and particles absorption coefficient respectively, λ_1 and λ_2 are the minimum and maximum wavelength of the response spectrum of the CCD camera.

From Eqs. (3)–(5), the following equation can be obtained:

$$E_{i\to j} = E_i\cdot D_{i\to j} = 4\Delta V_i\cdot D_{i\to j}\cdot\int_{\lambda_1}^{\lambda_2}(\alpha_{g,i}+\alpha_{p,i})e_{b\lambda,i}\,d\lambda \tag{6}$$

The response wavelength of the general CCD camera is within 0.4–0.7 μm which is the wavelength range of visible light. Spectral absorption coefficients of CO_2 can be considered to be zero in this wavelength range. The radiative properties of particles can be considered to be independent of the visible wavelength for large particles. Based on above analysis, Eq. (6) can be simplified and the following equation can be gained

$$E_{i\to j} = 4\Delta V_i\cdot\alpha_{p,i}\cdot D_{i\to j}\cdot\int_{\lambda_1}^{\lambda_2}e_{b\lambda,i}\,d\lambda = A_{i\to j}\cdot T_{Ei} \tag{7}$$

$$\text{where}\quad A_{i\to j} = 4\Delta V_i\cdot\alpha_{p,i}\cdot D_{i\to j} \tag{8}$$

$$\text{and}\quad T_{Ei} = \int_{\lambda_1}^{\lambda_2}e_{b\lambda,i}\,d\lambda \tag{9}$$

Then the following equations can be deduced according to Eqs. (2) and (7):

$$\begin{aligned} \sum_{i=1}^{N}(A_{i\to 1}\cdot T_{Ei}) &= P_1 \\ \sum_{i=1}^{N}(A_{i\to 2}\cdot T_{Ei}) &= P_2 \\ &\vdots \\ \sum_{i=1}^{N}(A_{i\to M}\cdot T_{Ei}) &= P_M \end{aligned} \tag{10}$$

Rewrite Eq. (10) in the matrix equation form

$$\boldsymbol{A}\boldsymbol{T}_E = \boldsymbol{E}, \boldsymbol{A}\in\boldsymbol{R}^{M\times N},\quad \boldsymbol{T}_E\in\boldsymbol{R}^N,\quad \boldsymbol{E}\in\boldsymbol{R}^M \tag{11}$$

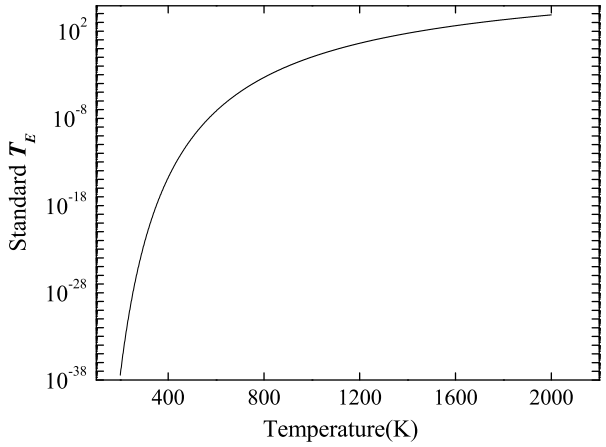

Fig. 3. Standard $\boldsymbol{T_E}$ under different temperatures.

where $\boldsymbol{A}$ is the coefficient matrix and can be obtained through Monte Carlo method, $\boldsymbol{T_E}$ is determined by Eq. (9), $\boldsymbol{E}$ is the radiative energy vector.

In the direct problem, for the known temperature field and radiative properties, $\boldsymbol{A}$ and $\boldsymbol{T_E}$ can be obtained through Monte Carlo method. The radiative energy received by CCD cameras at the boundary surfaces can be calculated by Eq. (11).

2.2. Inverse problem

For the inverse problem, the temperature field is regarded as unknown. The temperature field can be estimated by using the exit radiative energy vector $\boldsymbol{E}$ measured by CCD cameras.

The inverse problem is an ill-posed problem and Eq. (11) is an ill-posed matrix equation. In order to get stable and reasonable solutions, LSQR method is employed. LSQR method is one of the most efficient methods for the solution of large-scale ill-posed problems [31,32]. LSQR is analytically equivalent to the standard method of conjugate gradients, but processes more favorable numerical properties. The more details of the LSQR method can be available in Refs. [33,34].

After Eq. (11) is solved, temperature field can be obtained by Eq. (9). The values of standard $\boldsymbol{T_E}$ in Eq. (9) corresponding to different temperatures are calculated in advance, as shown in Fig. 3. Once $\boldsymbol{T_E}$ is obtained through inverse solution, three-dimensional temperature field can be immediately obtained according to Fig. 3.

3. Results and discussion

Errors could not only exist in radiative energy vector $\boldsymbol{E}$ obtained by CCD cameras but also exist in the coefficient matrix $\boldsymbol{A}$ due to some measuring inaccuracy, some fluctuations in radiative properties, some calculation imprecision and so on. So random errors of normal distribution with zero average value and mean square deviation σ_1 and σ_2 were added to the energy $\boldsymbol{E}$ and the coefficient matrix $\boldsymbol{A}$ in Eq. (11), respectively,

$$\boldsymbol{E}_{\text{measured},j} = (\mu + \sigma_1\xi)E_j + E_j \tag{12}$$

$$\boldsymbol{A}_{\text{err},n} = (\mu + \sigma_2\xi)A_n + A_n \tag{13}$$

where $E_{\text{measured},j}$ is the element of the energy vector $\boldsymbol{E}_{\text{measured}}$ with errors and $A_{\text{err},\,n}$ is the element of coefficient matrix $\boldsymbol{A}_{\text{err}}$ with errors. E_j is the element of the exact energy vector $\boldsymbol{E}$ and A_n is the element of exact coefficient matrix $\boldsymbol{A}$. Average value μ equals zero, ξ is a random variable of standard normal distribution and the probability lying in the range of $-2.576 < \xi < 2.576$ is 99%. $j = 1, 2, \ldots, M$; $n = 1, 2, \ldots, M \times N$.

To examine the accuracy and computational efficiency of the method developed in this paper, the following temperature field is adopted as the exact one in the media, as shown in Fig. 4. W, L, H of the enclosure are equal to 0.4 m and the CCD target plane is assumed to be divided into 30×30 pixel elements.

The above temperature field is not assumed arbitrarily. Firstly the CFD simulation was carried out for an actual pulverized coal-fired furnace and temperature filed was obtained. The temperature distribution near combustion burner region was adopted as the assumed exact temperature field in this paper. From Fig. 4 it is worth noting that the temperature field is very complicated and the range of temperature is between 800 K and 1800 K which represents the temperature range for combustion conditions found in typical fires and furnaces [35].

The reconstruction error for the temperature field and the relative error for the temperature in each volume element are defined as

$$E_{\text{recon}} = 100\sqrt{\frac{1}{N}\sum_{i=1}^{N}(T_i^{\text{recon}} - T_i^{\text{exact}})^2} \Big/ \left(\frac{1}{N}\sum_{i=1}^{N} T_i^{\text{exact}}\right) \tag{14}$$

$$E_{\text{rel},i} = 100\frac{|T_i^{\text{recon}} - T_i^{\text{exact}}|}{T_i^{\text{exact}}} \tag{15}$$

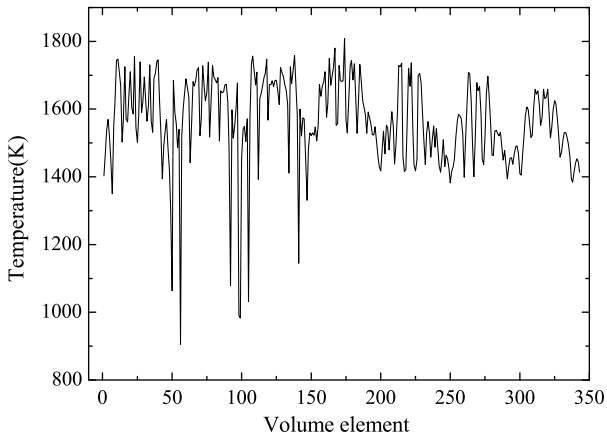

Fig. 4. Exact temperature field in participating media.

where T_i^{recon} and T_i^{exact} represent reconstructed and exact temperature respectively, $i = 1, 2, \ldots, N$.

In the following three cases, the effects of measurement errors, combinations of CCD cameras, concentration distributions of particles, and coefficient fluctuating errors on the accuracy of the inverse problem were investigated. Firstly, in case 1 it is assumed that only measured exit radiative energy vector $\boldsymbol{E}$ has measurement errors. Then, in case 2 only coefficient matrix $\boldsymbol{A}$ in Eq. (11) has fluctuating errors. Finally, both measurement errors and coefficient fluctuating errors exist simultaneously in case 3.

3.1. Case 1

In this case, it is assumed that the coefficient matrix $\boldsymbol{A}$ has no fluctuating errors and only measured exit radiative energy vector has errors. The effects of measurement errors, the various combinations of CCD cameras, and concentration distributions of particles on the accuracy of estimation are examined. Due to the use of random errors adding to the exact solution of direct problem, all the reconstruction results are the average results of 100 samples.

3.1.1. Effects of various combinations of CCD cameras on reconstruction accuracy

Concentration distribution (1) is used. As shown in Fig. 5, six different combinations of CCD cameras are used, and the locations of CCD cameras from the number (1) to (8) are illustrated in Fig. 1. It is found that with different measurement errors, the results from eight CCD cameras are the best and the results from one CCD camera are the worst. The reconstruction errors decrease with the increase of CCD camera quantity under certain fixed measurement error. The accuracy of estimation decreases as the measurement errors increase for all six combinations. For the same quantity of CCD cameras, for example, for combinations of four CCD cameras (1)(2)(3)(4) and (1)(3)(6)(8), reconstruction error has some differences between two combinations with no measurement error but there are no obvious differences with mean square deviation of 0.005 and 0.01. As more CCD cameras are used for receiving the radiative energy exiting the boundaries, more radiative information of the three-dimensional participating media can be obtained and better results may be expected.

3.1.2. Reconstruction results from eight CCD cameras with exact and noisy data

Let us examine the reconstruction results for eight CCD cameras carefully. Concentration distribution (1) is used. LSQR method used in this paper is an iteration method. Reconstruction errors under different iteration times are calculated in order to determine the best iteration times, as shown in Fig. 6. It is noted that for each curve there is a lowest point and the iteration times corresponding to this point is the best iteration times.

Reconstructed temperature fields are illustrated in Fig. 7 with no measurement errors and with mean square deviation of 0.01. The agreement between the estimated and the exact temperature field is excellent with no measurement errors. Only few differences can be observed with mean square deviation of 0.01. The relative errors between the reconstructed temperature and the exact one for each volume element have also been calculated and shown in Fig. 8. It can be seen that the relative errors with no measurement errors are quite small and most of those with mean square deviation of 0.01 can be maintained at a low level. Few points cannot be reconstructed well because the temperature values of these points were lower and reconstruction for these points can be influenced more easily by measurement errors. The overall reconstruction results indicate that the inverse method developed in this paper can obtain

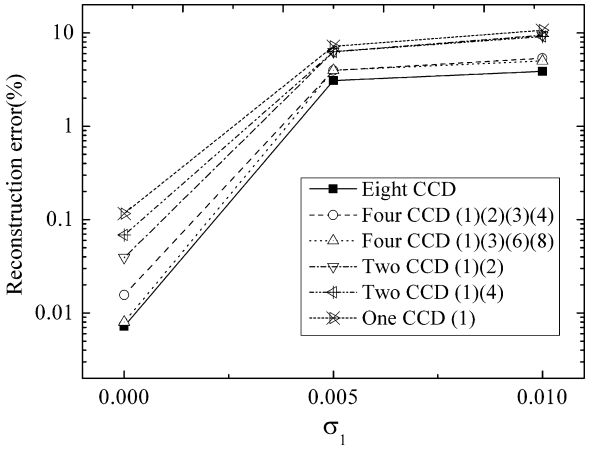

Fig. 5. Reconstruction errors for various combinations of CCD cameras and different measurement errors.

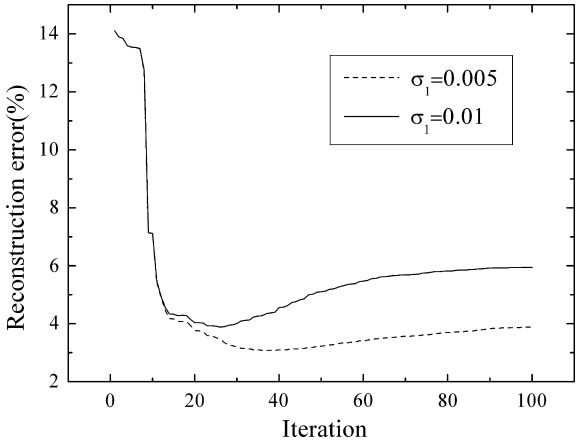

Fig. 6. Reconstruction errors varying with iteration times under two kinds of measurement errors.

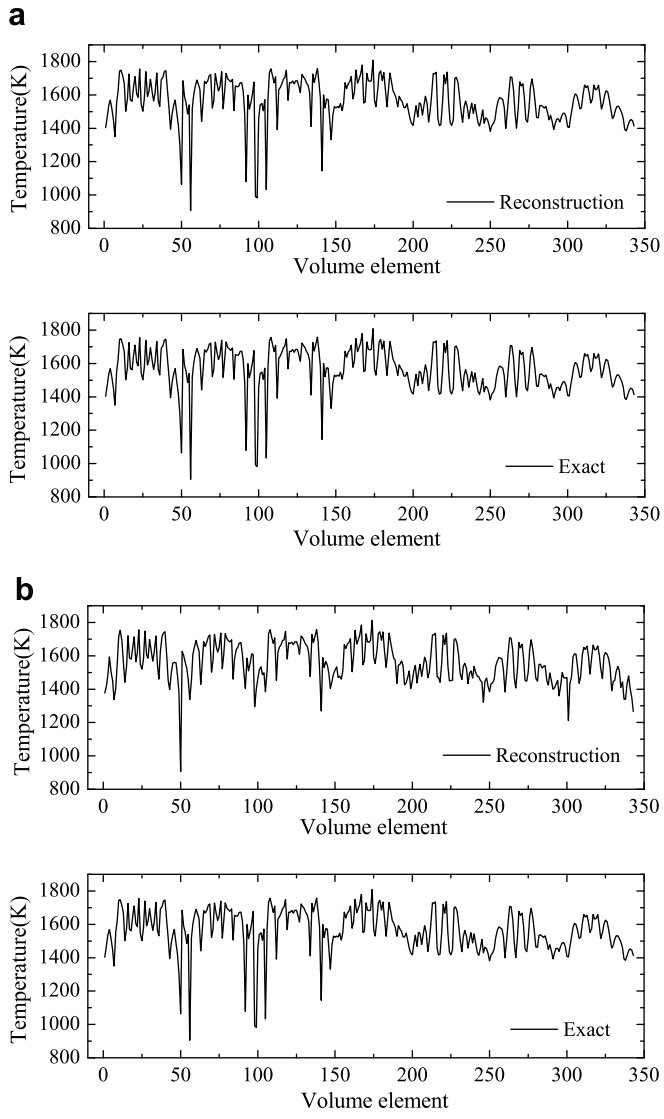

Fig. 7. Reconstructed temperature fields for different measurement errors, (a) $\sigma_1 = 0$ and (b) $\sigma_1 = 0.01$.

accurate and reasonable temperature fields, even with noisy input data.

3.1.3. Effects of concentration distributions of particles on estimation accuracy

In this section, the reconstruction errors under concentration distribution (2) from four CCD cameras (1)(3)(6)(8) are investigated.

The comparison of results between concentration distributions (1) and (2) is shown in Fig. 9. It is found that with different measurement errors, reconstruction errors of concentration distribution (2) are larger than those of concentration distribution (1). The reason may be that the average concentration of particles in concentration distribution (2) is larger than that in concentration distribution (1) and average optic thickness is larger in concentration distribution (2). The radiative information of three-dimensional participating media received by CCD cameras may be less

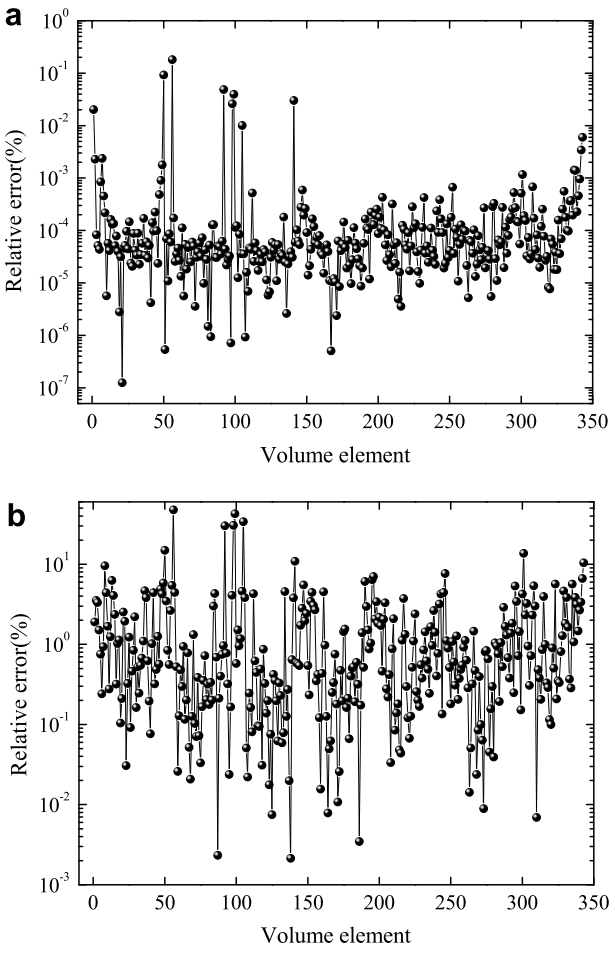

Fig. 8. Relative error for each volume element, (a) $\sigma_1 = 0$ and (b) $\sigma_1 = 0.01$.

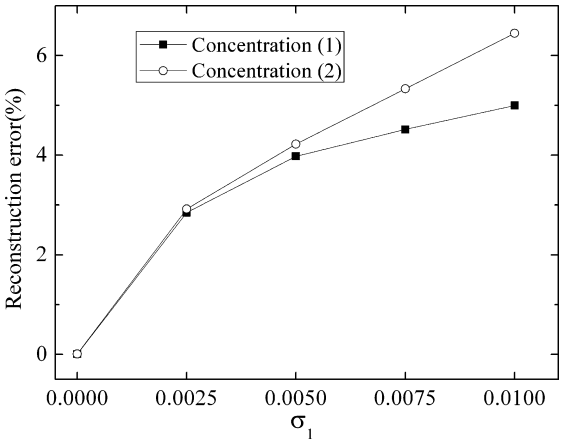

Fig. 9. Effects of concentration distributions of particles on the accuracy of estimation.

in concentration distribution (2) and reconstruction errors accordingly become larger.

Moreover, it also can be seen that as measurement error increases, the reconstruction error for concentration distribution (2) increases faster and larger than that for concen-

tration distribution (1), which may be due to the ill-posed characteristics of the inverse problem and for larger measurement errors, the accuracy and stability of reconstruction are influenced more easily by the errors.

3.2. Case 2

The effects of the coefficient matrix errors on the accuracy of the inverse estimation are examined. It is assumed that only coefficient matrix has fluctuating errors and there are no measurement errors in this case. Eight CCD cameras and concentration distribution (1) are used.

The reconstruction errors with various mean square deviations are shown in Fig. 10 and for comparison, some results for eight CCD cameras in case 1 are also included. It is worth noting that as the increase of mean square deviation, the reconstruction error for eight CCD cameras in case 1 increases faster and larger compared with that of case 2. This reveals that the effects of coefficient matrix errors could be less compared with the effects of the measurement errors on the accuracy of estimation.

Moreover, Fig. 10 also implies that, in order to improve the accuracy of the reconstruction of the temperature field, the measurement errors of the exit radiative energy should be confined within an appropriate range.

3.3. Case 3

In the practical processes of measurement and inverse solution, both measurement errors and coefficient fluctuating errors may exist at the same time. Concentration distribution (1) is used and the results are shown in Fig. 11.

It can be seen that, with two kinds of measurement errors, the reconstruction errors increase with coefficient fluctuating errors but the difference between reconstruction error of $\sigma_1 = 0.005$ and that of $\sigma_1 = 0.01$ becomes smaller and smaller. As σ_2 equals 0.005, the difference between reconstruction error of $\sigma_1 = 0.005$ and that of $\sigma_1 = 0.01$ is 0.8%, whereas σ_2 equals 0.05, the difference decreases

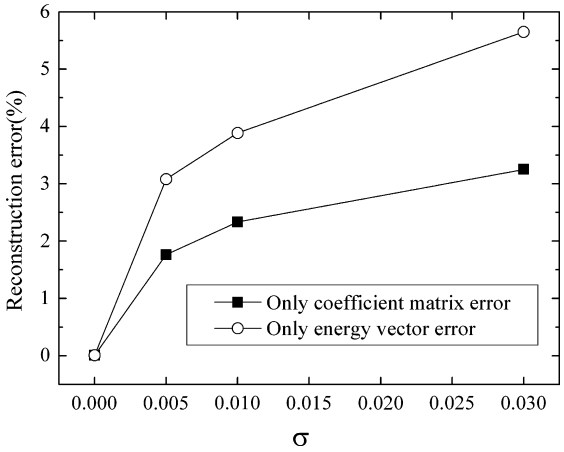

Fig. 10. Effects of two kinds of errors separately on the accuracy of estimation.

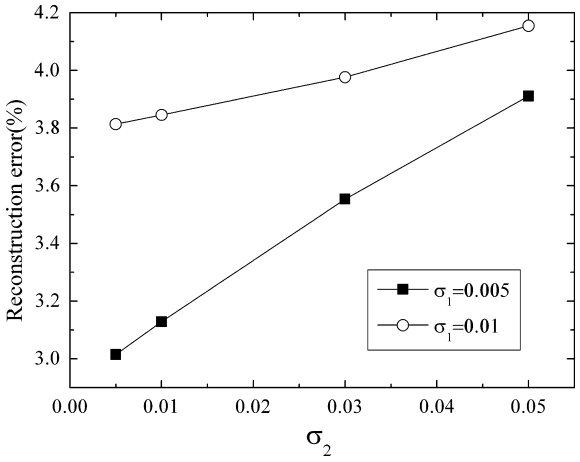

Fig. 11. Effects of measurement errors and coefficient errors on the accuracy of estimation simultaneously.

to 0.2%. From this point of view, for larger coefficient errors, measurement errors have a relatively less influence on the accuracy of reconstruction, which is also true for larger measurement errors. For larger measurement errors ($\sigma_1 = 0.01$), the reconstruction error increases much slowly with σ_2, that is, σ_2 increasing from 0.005 to 0.05, the reconstruction error for $\sigma_1 = 0.01$ increases from 3.8% to 4.1% but the reconstruction error for $\sigma_1 = 0.005$ increases from 3.0% to 3.9%. This also implies that the restraining effects of LSQR method on lager errors are more obvious so that reconstruction errors of inverse problem cannot increase quickly with the measurement errors and coefficient errors.

4. Conclusions

A method is presented for determining the three-dimensional temperature field in an inhomogeneous, absorbing, emitting and anisotropically scattering media of known radiative properties from the knowledge of the exit radiative energy received by CCD cameras at boundary surfaces. In this study, the forward Monte Carlo method is employed to describe the radiative energy propagation and LSQR method is introduced to solve the ill-posed matrix equation. Although the temperature is a function of space variables, only the measurements of exit radiative energy at the boundary surfaces are required. Both measurement errors and coefficient fluctuating errors are considered. The results show that the present technique is robust and yields accurate three-dimensional temperature field for the exact and noisy input data.

Acknowledgements

The supports of this study by the State Key Program of National Natural Science Foundation of China (Grant No. 60534030) and Program for Changjiang Scholars and Innovative Research Team in University (Grant No. IRT0434) are gratefully acknowledged.

References

[1] R. Viskanta, M.P. Mengüç, Radiation heat transfer in combustion systems, Prog. Energy Combust. Sci. 13 (1987) 97–160.

[2] N.J. McCormick, Inverse radiative transfer problems: a review, Nucl. Sci. Eng. 112 (1992) 185–198.

[3] C.H. Ho, M.N. Özişik, An inverse radiation problem, Int. J. Heat Mass Transfer 32 (2) (1989) 335–341.

[4] C.H. Ho, M.N. Özişik, Inverse radiation problems in inhomogeneous media, JQSRT 40 (5) (1988) 553–560.

[5] W.L. Dunn, Inverse Monte Carlo solutions for radiative transfer in inhomogeneous media, JQSRT 29 (1) (1983) 19–26.

[6] S. Subramaniam, M.P. Mengüç, Solution of the inverse radiation problem for inhomogeneous and anisotropically scattering media using Monte Carlo technique, Int. J. Heat Mass Transfer 34 (1) (1991) 253–266.

[7] A.J.S. Neto, M.N. Özişik, An inverse problem for simultaneous estimation of radiation phase function, albedo and optical thickness, JQSRT 53 (4) (1995) 397–409.

[8] H.Y. Li, A genetic algorithm for inverse radiation problems, Int. J. Heat Mass Transfer 40 (7) (1997) 1545–1549.

[9] K.W. Kim, S.W. Baek, M.Y. Kim, H.S. Ryou, Estimation of emissivities in a two-dimensional irregular geometry by inverse radiation analysis using hybrid genetic algorithm, JQSRT 87 (2004) 1–14.

[10] H.M. Park, T.Y. Yoon, Solution of the inverse radiation problem using a conjugate gradient method, Int. J. Heat Mass Transfer 43 (2000) 1767–1776.

[11] H.Y. Li, M.N. Özişik, Identification of the temperature profile in an absorbing, emitting, and isotropically scattering medium by inverse analysis, J. Heat Transfer 114 (1992) 1060–1063.

[12] H.Y. Li, M.N. Özişik, Inverse radiation problem for simultaneous estimation of temperature profile and surface reflectivity, J. Thermophys. Heat Transfer 7 (1) (1993) 88–93.

[13] C.E. Siewert, An inverse source problem in radiation transfer, JQSRT 50 (1993) 603–609.

[14] C.E. Siewert, A radiative-transfer inverse-source problem for a sphere, JQSRT 52 (1994) 157–160.

[15] H.Y. Li, Estimation of the temperature profile in a cylindrical medium by inverse analysis, JQSRT 52 (1994) 755–764.

[16] L.H. Liu, H.P. Tan, Q.Z. Yu, Simultaneous identification of temperature profile and wall emissivities in one-dimensional semi-transparent medium by inverse radiation analysis, Numer. Heat Transfer, Part A 36 (1999) 511–525.

[17] L.H. Liu, Simultaneous identification of temperature profile and absorption coefficient in one-dimensional semitransparent medium by inverse radiation analysis, Int. Commun. Heat Mass Transfer 27 (5) (2000) 635–643.

[18] L.H. Liu, H.P. Tan, Q.Z. Yu, Inverse radiation problem of sources and emissivities in one-dimensional semitransparent media, Int. J. Heat Mass Transfer 44 (2001) 63–72.

[19] H.Y. Li, Inverse radiation problem in two-dimensional rectangular media, J. Thermophys. Heat Transfer 11 (4) (1997) 556–561.

[20] H.Y. Li, A two-dimensional cylindrical inverse source problem in radiative transfer, JQSRT 69 (2001) 403–414.

[21] L.H. Liu, H.P. Tan, Q.Z. Yu, Inverse radiation problem of temperature field in three-dimensional rectangular furnaces, Int. Commun. Heat Mass Transfer 26 (2) (1999) 239–248.

[22] L.H. Liu, H.P. Tan, Inverse radiation problem in three-dimensional complicated geometric systems with opaque boundaries, JQSRT 68 (2001) 559–573.

[23] J.R. Howell, The Monte Carlo method in radiative heat transfer, J. Heat Transfer 120 (1998) 547–560.

[24] T.W. Tong, R.D. Skocypec, Summary on comparison of radiative heat transfer solutions for a specified problem, Developments in Radiative Heat Transfer, ASME HTD 203 (1992) 253–264.

[25] J.T. Farmer, J.R. Howell, Monte Carlo prediction of radiative heat transfer in inhomogeneous, anisotropic, nongray media, J. Thermophys. Heat Transfer 8 (1) (1994) 133–139.

[26] M.F. Modest, Radiative Heat Transfer, McGraw-Hill, New York, 1993, pp. 383–437.

[27] D.G. Goodwin, M. Mitchner, Flyash radiative properties and effects on radiative heat transfer in coal-fired system, Int. J. Heat Mass Transfer 32 (4) (1989) 627–638.

[28] C. Kim, N. Lior, Easily computable good approximations for spectral radiative properties of particle-gas components and mixture in pulverized coal combustors, Fuel 74 (12) (1995) 1891–1902.

[29] J.G. Marakis, C. Papapavlou, E. Kakaras, A parametric study of radiative heat transfer in pulverized coal furnaces, Int. J. Heat Mass Transfer 43 (2000) 2961–2971.

[30] M.P. Mengüç, R. Viskanta, Radiative transfer in three-dimensional rectangular enclosure containing inhomogeneous, anisotropically scattering media, JQSRT 33 (6) (1985) 533–549.

[31] S. Morigi, L. Reichel, F. Sgallari, F. Zama, Iterative methods for ill-posed problems and semiconvergent sequences, J. Comput. Appl. Math. 193 (2006) 157–167.

[32] J. Baglama, L. Reichel, Decomposition methods for large linear discrete ill-posed problems, J. Comput. Appl. Math. 198 (2007) 332–343.

[33] C.C. Paige, M.A. Saunders, LSQR: an algorithm for sparse linear equations and sparse least squares, AMC Trans. Math. 8 (1) (1982) 43–71.

[34] C.C. Paige, M.A. Saunders, LSQR: sparse linear equations and least squares problems, AMC Trans. Math. 8 (2) (1982) 195–209.

[35] W.L. Grosshandler, A.T. Modak, Radiation from nonhomogeneous combustion products, in: 18th Symp. (Int.) on Combustion, The Combustion Institute, 1981, pp. 601–609.